AAS 07-188

THERMOSPHERIC DENSITY MODEL INCLUDING MAGNETOSPHERIC ENERGY SOURCES AT QUIET TIMES

Kenneth Moe* and Mildred M. Moe*

Recent measurements by the accelerometer on the CHAMP Satellite have confirmed that energy flows into the thermosphere from the dayside cusps of the magnetosphere at all times. This energy source produces dayside density enhancements at high latitudes. The semi-empirical model described here can reproduce these density increases. The parameters in the model were originally determined 30 years ago, but can now be improved by using the densities measured by the CHAMP/STAR accelerometer, the semiannual variation improved by Bruce Bowman, and the UV energy source provided by Kent Tobiska. Recent improvements in determining satellite drag coefficients can enable the model to provide absolute densities.

HISTORICAL INTRODUCTION

When the science of spectroscopy was developed in the 19th and 20th centuries, it was discovered that solar ultraviolet radiation heats, dissociates, and ionizes the upper atmosphere[1]. Great auroral displays had been observed for millennia, and there were various theories about their cause[2]. In the 1930s Sydney Chapman and V. C. A. Ferraro were the first to show how streams of ions emitted from the solar corona could interact with the earth's magnetic field to produce a magnetosphere[3]. When satellites began flying, Chapman pointed out that energy from the solar corona continuously flows into the interplanetary gas, and part of this energy flows into the Earth's upper atmosphere at all times[4]. Yet little was known about how solar corpuscular energy entered the Earth's magnetosphere and thermosphere, so the theoretical static diffusion models of Marcel Nicolet and Philip Mange simply assumed that solar UV radiation was the only energy source[5,6] for the thermosphere. This idea was carried into the early thermospheric models that fitted satellite drag data to the static diffusion equations. However, Julius Bartels, who was a world authority on geomagnetism, insisted that there was also corpuscular energy flowing into the thermosphere at high latitudes[7].

As the resolution of satellite drag data improved, Luigi Jacchia and Jack Slowey were able to detect the corpuscular energy that enters the atmosphere during geomagnetic storms[8]. Paetzold's model was the first to incorporate a density increase caused by geomagnetic heating[9]. By 1964, the static diffusion models of Harris and. Priester[10] and Jacchia[11] also included a geomagnetic storm effect . Jacchia introduced

*Senior Scientist, Space Environment Technologies, 23 Purple Sage, Irvine, CA 92603

the geomagnetic storm effect into his static diffusion model by increasing the exospheric temperature as a function of the geomagnetic indices, Ap or Kp[8,11].

Nevertheless, the effect of corpuscular energy on the thermospheric density at quiet times was not understood until the Canadians flew their Alouette and ISIS Satellites[12-17]. Thermospheric densities derived from the recent CHAMP/STAR accelerometer data[18-20] confirm the presence of the dayside high-latitude density enhancements which result from energy flowing from the magnetosphere into the thermosphere during geomagnetically quiet times. The location of the density bulge is collocated with the regions of red airglow[14], the locations of electron concentration peaks in the high-latitude ionosphere[15,16], and the regions of particle precipitation into the dayside thermosphere from several parts of the magnetosphere[12-13,21-22]. The bulge is centered on the downward projection of the dayside magnetospheric cusp[17].

EARLY EVIDENCE FROM SATELLITE DRAG

The early evidence for the thermospheric polar density enhancement came in the 1960s, when the Air Force started launching polar satellites. At first the bulge was inferred from orbital decay data by Rodney Jacobs[23]. Later Barbara Ching demonstrated that she could improve the correlation between polar satellite drag data and the Jacchia density model by replacing the subsolar density bulge by a high-latitude bulge[24]. Toward the end of the decade, the Air Force placed an accelerometer on the polar satellite, LOGACS[25,26]. That experiment defined the bulge more clearly, and confirmed that the high latitude bulge is larger in magnitude than the subsolar density bulge. Most of the information derived from Air Force polar satellites was unknown to the aeronomic community until Col. Leonard DeVries convinced Gen. Samuel Phillips to declassify it in 1971 (Reference 27). Because the polar density bulge was unknown to the developers of early static diffusion models that fitted satellite data, the models of Jacchia[11], Harris and Priester[10], and Paetzold[9] did not include such a density bulge at quiet times. .

ALOUETTE AND ISIS

Early in the 1960s, the Canadians began to fly their Alouette Satellites, which carried an ionosonde that looked down on the ionosphere in the Northern Hemisphere. These ionosondes sometimes revealed sudden increases in electron density unlike the patterns seen at lower latitudes[15,16]. To understand the causative processes, the Canadians then flew the ISIS satellites, which gathered valuable data on topside ionospheric electron concentrations, the red airglow, and particle precipitation[12-16]. The reports of particle precipitation convinced us that the collaboration of a magnetospheric physicist was essential. Willard P. Olson examined the particle data. He used the ISIS measurements published by Heikkela and Winningham[13] to outline the region of particle precipitation[28]**.** It is idealized as a lunette-shaped region on the dayside shown as the shaded area in Figure 1. At the center of the figure is the geographic North Pole. Noon is at the bottom of the figure. The upper dashed circle is the locus of the magnetic pole as the earth rotates. At 23 hours UT, the magnetic pole is at the point labeled “23” on the upper circle. To find the center of the lunette arc, we must move 15^0 equatorward toward the

Sun, placing the center of the lunette at the point "23" on one of the lower circles which depend on season (winter in Figure 1).

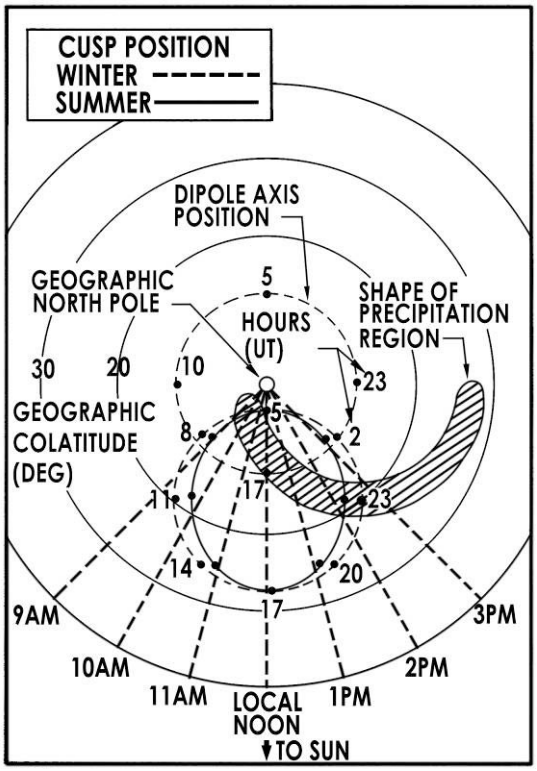

Figure 1 Willard Olson's Model of Dayside Cusp Precipitation

As the day progresses and the Earth rotates, the center of the lunette arc moves counterclockwise on one of the lower circles**.** Thus the region shifts around in local time and in geographic latitude and longitude. The lunette always faces the sun, with its wings pointing away from the sun. The center of the lunette arc coincides with the footprint of the magnetospheric dayside cusp. This is not to say that all the energy is coming from the cusp. Patrick Newell and his colleagues have discovered that many particles, especially those in the wings of the lunette, are coming from other parts of the magnetosphere, including the plasmasphere and tail[21,22]. Electric fields can also produce Joule heating in the ionized regions[29]. Whatever the combination of magnetospheric heating processes, the result is that this energized region is a persistent feature of the high-latitude structure at quiet times.

Airglow measurements are now important to density modelers, because the spectroscopic sensors SSUSI and SSULI are being flown on the DMSP Satellites to monitor thermospheric density[30]. Figure 2 shows the red airglow measured during the polar winter by Shepherd and Thirkettle on ISIS II. Olson's model of the particle precipitation from Figure 1 is shown shaded for comparison. Airglow measurements can help to improve the density model, and density measurements can help to validate and improve the SSUSI and SSULI measurements.

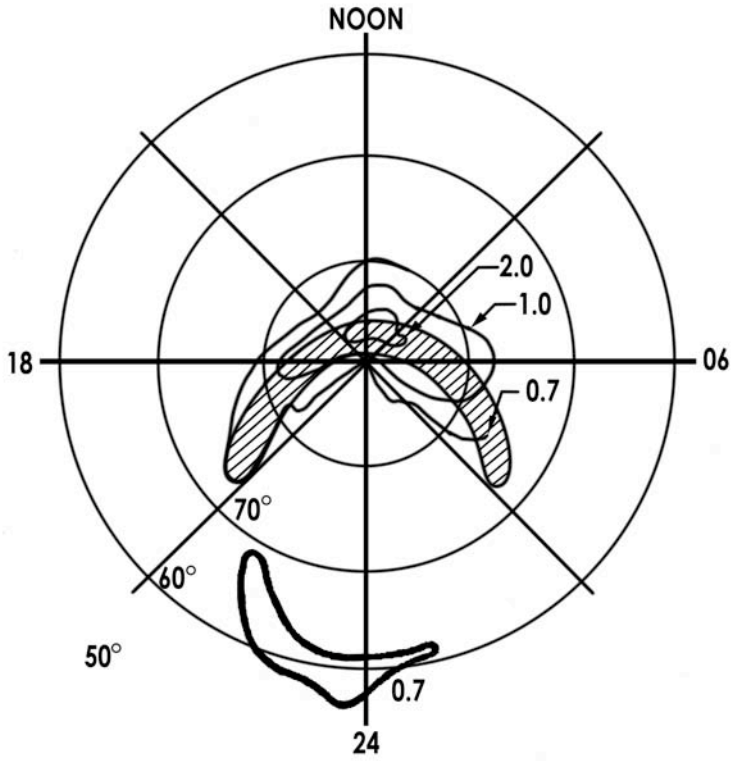

Figure 2 Red Airglow Compared with the Region of Dayside Precipitation
Shepherd and Thirkettle's contours of red airglow at the top resemble the shaded model of the dayside precipitation that excites the airglow during the polar night. The contour below is a nocturnal aurora caused by precipitation from the tail of the magnetosphere.

The ionosphere is an integral part of the thermosphere. The upper panel of Figure 3 shows the topside electron densities measured by the satellite Alouette I on a rare transit of the dayside precipitation region. The lower panel shows the neutral densities measured by the LOGACS accelerometer on pass 31, when it traversed the excited region. The composite figure is shown to demonstrate that the neutral response is spread out more in latitude than the ionospheric response. We believe this spread of the neutral response is caused by the longer time for molecular motions and thermal conduction than the lifetime of electrons. The neutral densities calculated from the Jacchia 1970 model and the present model are also shown for comparison with the LOGACS measurements. This comparison illustrates the importance of including the cusp-related energy source in density modeling. All of these measurements and models refer to geomagnetically quiet times.

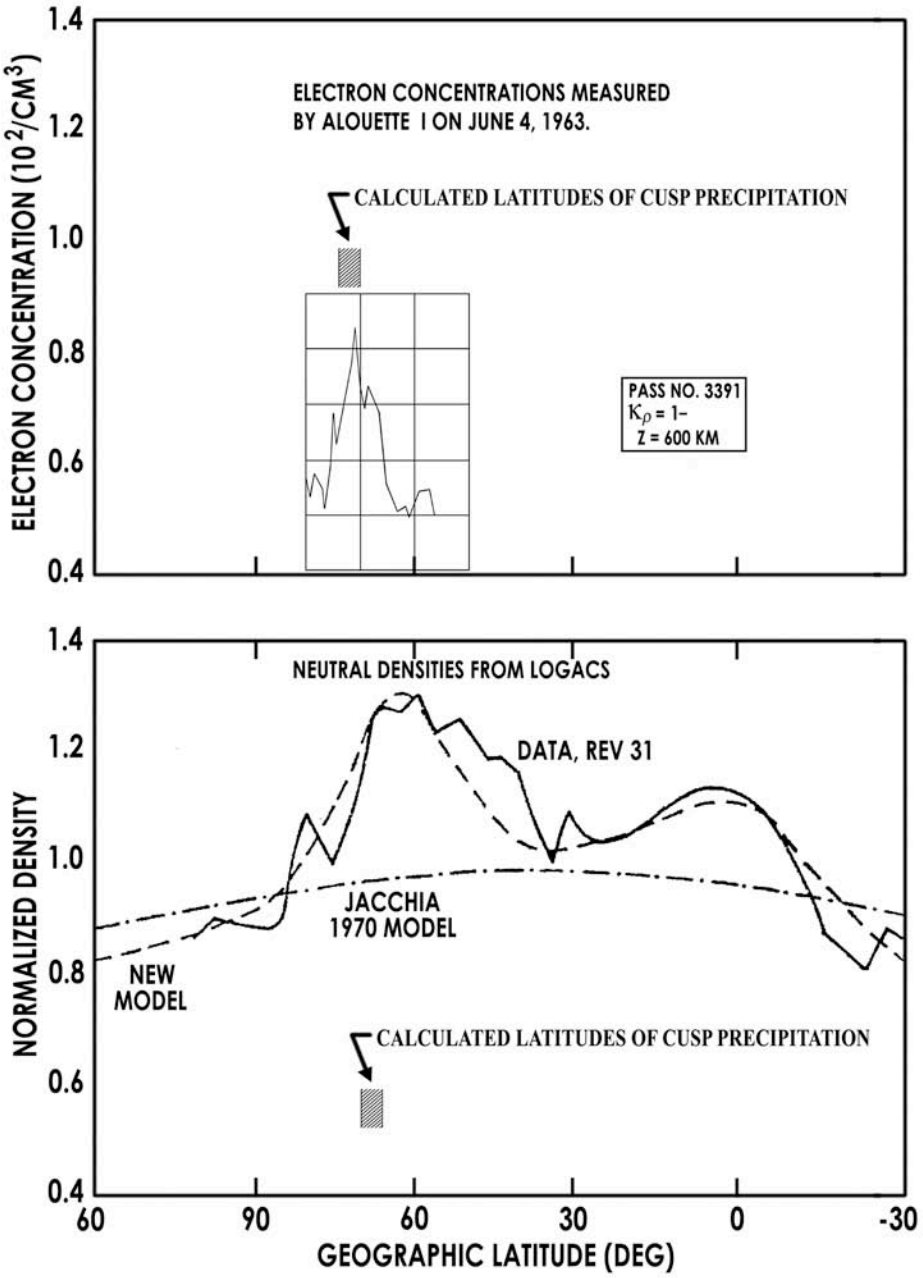

Figure 3 Cusp-Related Enhancements of the Electron and Neutral Densities

The upper panel shows the distribution of electron densities measured on Pass 3391 of Alouette 1 as a function of latitude. The lower panel shows the neutral densities measured by LOGACS on orbit 31as a function of latitude. In both panels, the shaded areas indicate the location of the modeled precipitation region. The neutral densities calculated from Jacchia's model and the present model are also shown.

THE SPADES SATELLITE

Figure 4 shows an example of density measurements made by the SPADES satellite, which carried a spinning pressure gauge[31,32]. The measurements in this figure were made as the satellite passed through the 400 km level in the Southern Hemisphere winter. Since there was no direct UV radiation, the energy was coming mostly through the magnetosphere. The measured density is plotted against geomagnetic colatitude**.** The density is given as a ratio relative to a static mid-latitude model, the spring/fall model for an exospheric temperature of 1000 K, from the U.S. Standard Atmosphere Supplements, 1966[33]. The darkened region displaced 15 degrees from the dipole is where the lunette model places the energized region**.** The numbers 45, 57, etc. refer to the orbital revolution number. The individual points represent densities derived from a single spin period of the pressure gauge. Whereas the energized region related to particle precipitation is narrow, the neutral density response is broad. One might expect this difference, because the times for thermal conduction and mass motions are hours, while the times even of forbidden excited transitions are seconds.

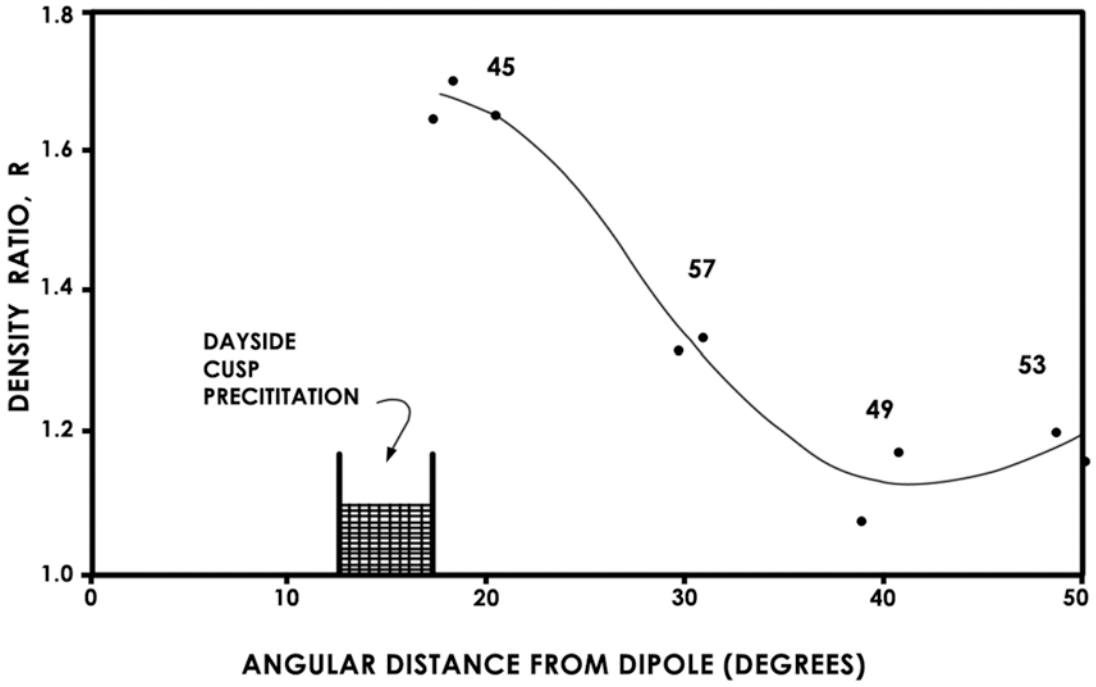

Figure 4 Densities Measured by the SPADES Satellite near the Southern Cusp

DEVELOPMENT OF AN EMPIRICAL MODEL INCLUDING THE CUSPS

Based upon the overwhelming evidence from satellite density measurements, electron concentration measurements, red airglow observations, and measurements of particle precipitation through the dayside cusp regions, an empirical model of the neutral density of the thermosphere was developed[34,35]. The neutral density is expressed as a sum of two parts: The first term ρ_u describes the combined effects of the solar ultra-violet heating and various other contributions like the semi-annual variation; the second term $\Delta\rho$ gives the contribution to the density associated with particle precipitation and joule heating coming from magnetospheric sources during times of low geomagnetic activity. The region of density enhancement at high latitudes is associated with the lunette shaped regions related to the dayside cusps. Therefore the model produces a density distribution which depends on universal time as well as on other variables like altitude, latitude, local time, and the solar UV energy source.

THE DENSITY FUNCTION *

The density ρ is expressed as a function of altitude z, geographic co-latitude θ, geographic longitude φ, universal time T, day of the year D, and the measure of the decimetric solar flux F:

$$\rho\,(z, \theta, \varphi, T, D, F) \;=\; \rho_u + \Delta\rho$$

where $\rho_u = \rho_0\,(z, F)\;\; B\,(z, \theta, t)\; J\,(z, \theta, D)\;\; Q\,(z, D)$

and t is the local time, $t = T + \varphi/15^0$. The term $\rho_0\,(z, F)$ is an exponential function which gives the height dependence of the mean equatorial density, B (z, θ, t) gives the diurnal variation, J (z, θ, D) gives the latitudinal and seasonal dependence, and Q (z, D) expresses the semi-annual effect.

The density bulges at high latitudes were constructed by centering them on the locations of the dayside cusps as modeled by Olson[28]. Since the density bulges are wider than the regions of particle precipitation, they have been approximated by a function suggested by observation of atmospheric densities at high latitudes:

$$\Delta\rho = \;\; \rho_0\,(z, F)\; C(\,z,\;\Delta\varepsilon\,)$$

where C(z, $\Delta\varepsilon$) is a function of the angular distance $\Delta\varepsilon$ of the point of observation from the central arc of the lunette-shaped precipitation region. It involves the geomagnetic coordinates of the point of observation, and indirectly the universal time.

The numerical values of the parameters in this semi-empirical model were originally determined 30 years ago from density data collected by the Bell-MESA accelerometer on

---

* A table of Notation appears near the end of this paper.

the LOGACS satellite and the pressure gauge on the SPADES satellite. As an example of the model output, we show in Figure 5 a Mercator projection of the global density distribution at a time of moderate solar activity. The densities are plotted against geographic east longitude and geographic latitude. At 12 hours UT, noon is at zero longitude while the north magnetic pole is eastward at about 290 degrees. The season is approaching northern summer, in late May. Notice that the maximum subsolar density is north of the equator. The high-latitude maximum is about 20 % higher than the subsolar maximum. As time progresses, the high-latitude bulge will shift relative to the subsolar bulge. It will shift in geographic latitude as well as in local time. This tells us that we cannot simply use local time and geographic latitude for a complete description of the thermospheric density distribution. We must include the shifting magnetospheric source.

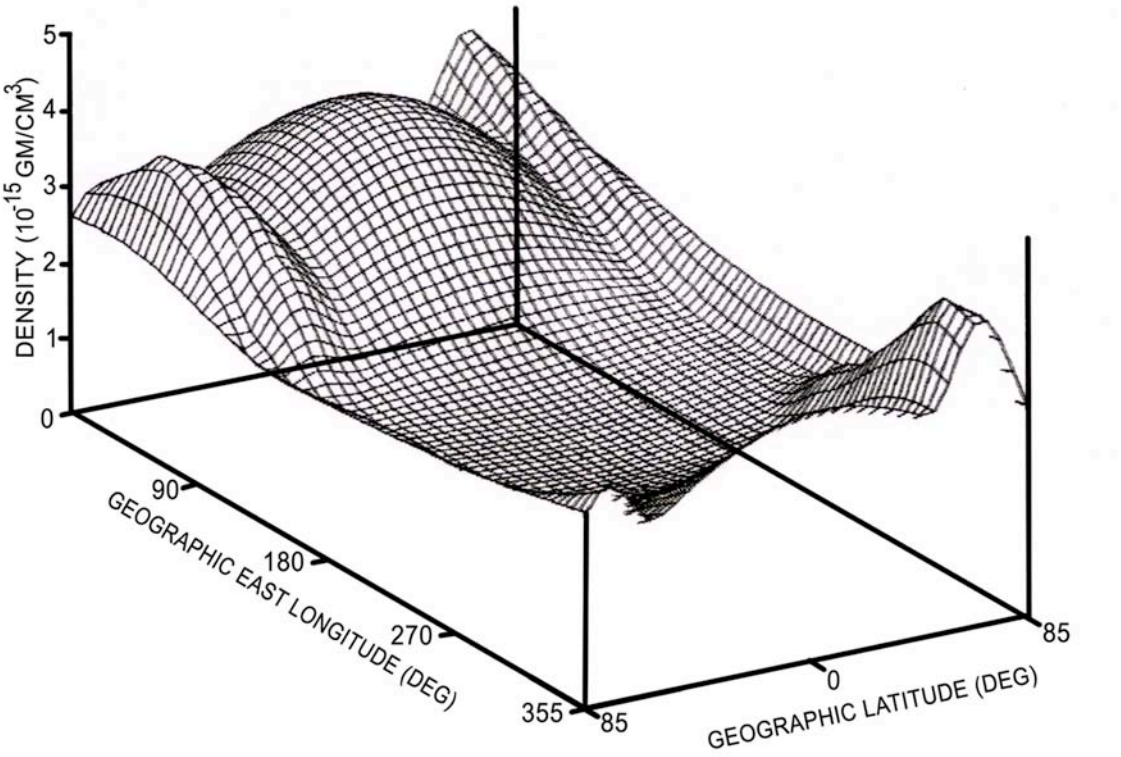

Figure 5 Global Density Distribution Including Cusp Energy Source

POSSIBILITIES FOR IMPROVEMENT

The parameters in the model can now be brought up to date by incorporating recent advances: The description of the semi-annual variation improved by Bruce Bowman[36] can be included in the function Q (z, D); the refinement of solar UV indices by Kent Tobiska[37] will alter the function ρ_0 (z, F). The large amount of precise density measurements made by the accelerometer on board the CHAMP Satellite[18-20] will provide a wealth of data to improve the parameters that describe the other functions in the model.

In the past, the drag coefficients of compactly-shaped satellites in free-molecular flow were often assumed to be 2.2 at all altitudes. That assumption has introduced biases in the Jacchia and MSIS density models. However, orbital measurements by satellites of special design have, in recent years, enabled better drag coefficients to be calculated for satellites of many shapes[38-40]. This development has made possible the calculation of absolute densities from drag data.

Some examples of drag coefficients are shown in Figure 6. These examples are: A smooth **sphere**; a **flat plate** at normal incidence to the airstream; the spinning **S3-1 Satellite**, which consisted of eight flat plates; and a **short cylinder** terminated by a flat plate that faces the airstream. A **long cylinder** that flew like an arrow would not fit on this graph, because it would have a drag coefficient between 3 and 4, depending mainly on the length-to-diameter ratio and the ambient temperature[41]. New measurements and calculations of drag coefficients will enable the present model to provide absolute densities up to an altitude of 500 km. See References 38 to 40 for details.

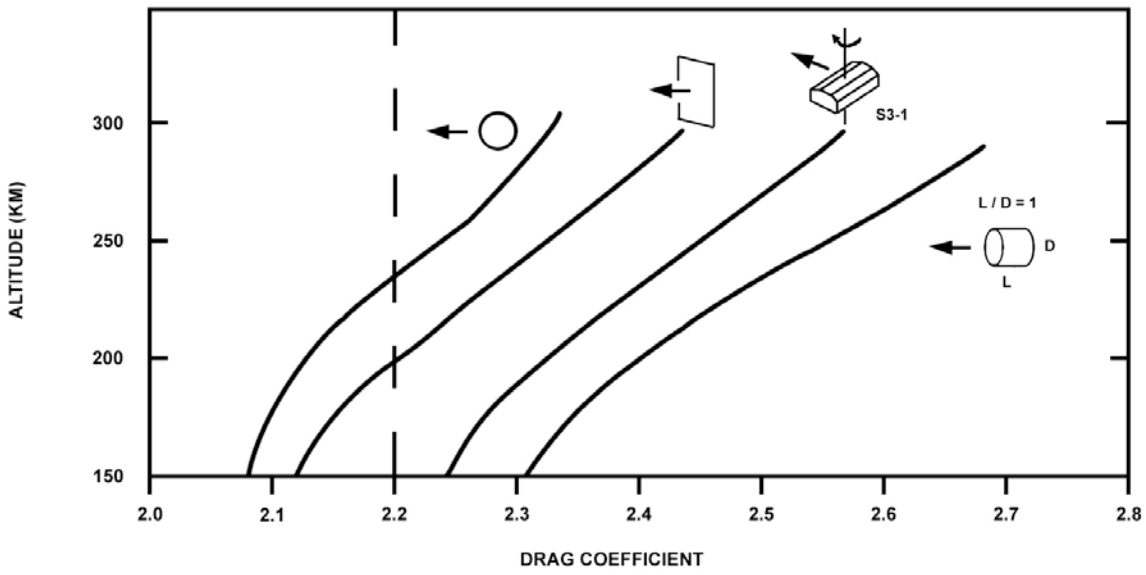

Figure 6 Drag Coefficients of Satellites in Low-Earth Orbit

SUMMARY

At geomagnetically quiet times there is a large magnetospheric energy source at high latitudes. It produces prominent dayside density enhancements which are dependent on universal time and are in the same locations as ionospheric electron density peaks, the red airglow, and particles precipitating from the magnetosphere. The semi-empirical model described here can reproduce the neutral density increases which appear at high latitudes in both hemispheres. Improved orbital data and analyses have recently become available: These can be used to improve the parameters in the model. Recent analyses of satellite drag coefficients can enable the model to provide absolute densities.

NOTATION

Ap = geomagnetic planetary amplitude
B = diurnal density variation
C = function of the distance from the central arc of the precipitation region
D = day of the year
F = decimetric solar flux
J = latitudinal and seasonal density variation
Kp = geomagnetic index
Q = semi-annual density variation
t = local time
T = universal time
z = altitude
$\Delta\rho$ = density enhancement at high latitudes
$\Delta\varepsilon$ = angular distance from central arc of the precipitation region
ρ = atmospheric density
ρ_u = atmospheric density without the high-latitude enhancement
ρ_0 = height dependence of the mean equatorial density
θ = geographic co-latitude
φ = geographic longitude

REFERENCES

1. S. K. Mitra, *The Upper Atmosphere*, The Royal Asiatic Society of Bengal, Calcutta, 1947, pp. 91-92 and 131-143.
2. S. K. Mitra, *The Upper Atmosphere*, The Royal Asiatic Society of Bengal, Calcutta, 1947, pp. 417-418.
3. S. Chapman and V. C. A. Ferraro, "Theory of Magnetic Storms", *Terr. Mag. and Atmos. Elec*., Vol. 36, 1931, pp. 77-97 and p. 171; also Vol. 37, 1932, p. 147 and p. 421.
4. S. Chapman, "The Thermosphere – The Earth's Outermost Atmosphere", in Ratcliffe, J. A. (Ed.), *Physics of the Upper Atmosphere*, Academic Press, NY and London, 1960, pp. 1-16.
5. M. Nicolet and P. Mange, J. Geophys. Res., Vol. 59, 1954, p. 16.
6. M. Nicolet., "Properties and Constitution of the Earth's Upper Atmosphere", in J. A. Ratcliffe (Ed.), *Physics of the Upper Atmosphere*, Academic Press, NY and London, 1960, pp. 17-71.
7. L. G. Jacchia, Private Communication, ca. 1970.

8. L. G. Jacchia and J. Slowey, "Atmospheric Heating in the Auroral Zones", *Smithsonian Astrophysical Observatory Spec. Rep. No. 136*, Cambridge, MA, 1963.
9. H.-K. Paetzold, "Model for the Variability of the Terrestrial Atmosphere After Satellite Acceleration", U. of Cologne, 1962; reprinted in *Flight Performance Handbook for Orbital Operations*, R. W. Wolverton, (Ed.), , John Wiley, NY and London, 1963, pp. 2-340 to 2-356.
10. I. Harris and W. Priester , "The Upper Atmosphere in the Range from 120 to 800 km", 1964; reprinted in *COSPAR International Reference Atmosphere*, North-Holland Publ. Co., Amsterdam, 1965.
11. L. G. Jacchia., "Static Diffusion Models of the Upper Atmosphere", *Smithsonian Astrophysical Observatory Spec. Rep. No. 170*, Cambridge, MA 1964.
12. J. D. Craven, "A Survey of Electron Fluxes", *J. Geophys. Res.*,Vol. 75, 1970, p. 2468.
13. W. J. Heikkila and J. D. Winningham, "Penetration of Magnetosheath Plasma to Low Altitudes through the Dayside Magnetospheric Cusps," *J. Geophys. Res.*, Vol. 76, 1971, p. 883.
14. G. G. Shepherd and E. W. Thirkettle, "Magnetospheric Dayside Cusp: A Topside View of its 6300 A Emission", *Science*, Vol. 180, 1973, p. 733.
15. K. l. Chan and L. Colin, "Global Electron Density Distributions from Topside Soundings", *Proc. IEEE,* Vol. 57, 1969, p. 990.
16. J. E. Titheridge, "Ionospheric Heating Beneath the Magnetospheric Cleft", *J. Geophys. Res.*, Vol. 81, 1976, p. 3221.
17. W. P. Olson and K. Moe, "Influence of Precipitating Charged Particles on the High-Latitude Thermosphere", *J. Atmos. Terr. Phys*. Vol. 36, 1974, pp. 1715-1726.
18. H. Luehr, M.Rother, W. Koehler, P. Ritter, and L. Grunwaldt, "Thermospheric Upwelling in the Cusp Region: Evidence from Champ Observations", *Geophys. Res. Lett*., Vol. 31, 2004, L06805.
19. S. Bruinsma, D. Tamagnan, and R. Biancale, "Atmospheric Densities Derived from CHAMP / STAR Accelerometer Observations", *Planet. Space Sci*., Vol. 52, 2004, pp. 297-312.
20. H. Liu, H. Luehr, V. Henize, and W. Koehler, "Global Distribution of the Thermospheric Total Mass Density Derived from CHAMP", *J. Geophys. Res*., Vol. 110, 2005, A04301.
21. P. T. Newell and C.-I. Meng, "The Cusp and the Cleft/Boundary Layer: Low Latitude Identification and Statistical Local Time Variation", *J. Geophys. Res*., Vol. 93, 1988, pp. 14,545-14549.
22. K. Liou, P. T. Newell, C.-I. Meng, T. Sotirelis, M. Brittnacher, and G. Parks, "Source Region of 1599 MLT Auroral Bright Spots: Simultaneous Polar UV- Images and DMSP Particle Data", *J. Geophys. Res*.," Paper No. 1999JA900290. 0148-0227/99/1999JA900290$09.00.
23. R. L. Jacobs, "Atmospheric Density Derived from the Drag of Eleven Low Altitude Satellites, *J. Geophys. Res*., Vol. 72, No.5, 1967, pp. 1571-1581.
24. B. K. Ching, "A Comparison of Drag Data with Several Model Atmospheres at Altitudes Below 200 km", *Report TOR 00059 (6110-01)* – 44, March 31, 1971. The Aerospace Corp., El Segundo, CA.
25 R. W. Bruce, "Upper Atmospheric Density Determination from LOGACS", in *The Low-G Accelerometer Calibration System*, Vol. II, Rept. No. TR-0074 (4260-10), Vol. II, The Aerospace Corp., El Segundo, CA, 1973, pp. 1-1 to 1-43..
26. L. L. DeVries, "Structure and Motion of the Thermosphere", in *Space Research XII*, Akademie-Verlag, Berlin, (GDR), Vol. b, 1972, p. 867.
27. L. L. DeVries, Private Communication, 1971.
28. W. P. Olson, "Corpuscular Radiation as an Upper Atmospheric Energy Source," in *Space Research XII*, Akademie-Verlag, Berlin (GDR), 1972, p. 1007.
29. K. D. Cole, 'Joule Heating of the Upper Atmosphere", *Australian J. of Physics*, Vol. 15, 1962, p. 223.
30. L. J. Paxton, et al., "Interactive Interpretation and Display of Far Ultraviolet Data", *Advances in Space Research*, Elsevier,UK, Vol. 22, no. 11, 1998, pp. 1577-1582. Elsevier.
31. V. L. Carter, B. K. Ching, and D. D. Elliott, "Atmospheric Density above 158 km Inferred from Magnetron and Drag Data from the Satellite OV1-15 (1968-059A)", *J Geophys. Res*., Vol. 74, 1969, p. 5083.
32. K. Moe, M. Moe, V. L. Carter, and M. B. Ruggera, Jr., "The Correlation of Thermospheric Densities with Charged Particle Precipitation Through the Magnetospheric Cleft", *J. Geophys. Res*., Vol. 82, 1977, pp. 3304-3306.
33. ESSA, NASA, and USAF, *US Standard Atmosphere Supplements, 1966*, Govt. Printing Office, Washington, D. C., 1966, pp. 39-47.

34. K. Moe and M. M. Moe, "A Dynamic Model of the Neutral Thermosphere," Report MDC G5891 to AF Office of Scientific Research under Contract F44620-72-CX-0084, McDonnell Douglas Astronautics Co., Huntington Beach, CA, 1975.
35. K. Moe, W. P. Olson, M. Moe, and G. Oelker, "A Thermospheric Model Which Includes Magnetospheric, Tropospheric, and Ultraviolet Energy Sources", *EOS, Trans of the Am. Geophys. Union*, Vol. 56, 1975, pp. 626-628.
36. B. R. Bowman, "The Semiannual Thermospheric Density Variation from 1970 to 2002 Between 200-1100 km", AAS2004-171, AAS Publications Office, P.O. Box 28130, San Diego, CA 92198, 2004.
37. W. K. Tobiska, "Advances in Solar Inputs for precision Orbit Determination", AAS 05-252, AAS Publications Office, P.O. Box 28130, San Diego, CA 92198, 2005.
38. K. Moe, and M. M. Moe, "Gas-Surface Interactions and Satellite Drag Coefficients", *Planet. Space Sci.,* Vol. 53, 2005, pp. 793-801.
39. B. R. Bowman and K. Moe, "Drag Coefficient Variability at 175-500 km from the Orbit Decay Analysis of Spheres", AAS 2005-257, AAS Publications Office, PO Box 28130, San Diego, CA 92198, 2005.
40. K. Moe and B. R. Bowman, "The Effects of Surface Composition and Treatment on Drag Coefficients of Spherical Satellites", AAS 2005-258, AAS Publications Office, PO Box 28130, San Diego, CA 92198, 2005.
41. L. H. Sentman, "Comparison of the Exact and Approximate Methods for Predicting Free-Molecular Aerodynamic Coefficients", *Am. Rocket Soc. J.*, Vol. 31, 1961, pp. 1576-1579.